World Academy of Science, Engineering and Technology
International Journal of Electronics and Communication Engineering
Vol:2, No:12, 2008

Performance Analysis of an Adaptive Threshold Hybrid Double-Dwell System with Antenna Diversity for Acquisition in DS-CDMA Systems

H. Krouma, M. Barkat, K. Kemih, M. Benslama, and Y. Yacine

***Abstract*—**In this paper, we consider the analysis of the acquisition process for a hybrid double-dwell system with antenna diversity for DS-CDMA (direct sequence-code division multiple access) using an adaptive threshold. Acquisition systems with a fixed threshold value are unable to adapt to fast varying mobile communications environments and may result in a high false alarm rate, and/or low detection probability. Therefore, we propose an adaptively varying threshold scheme through the use of a cell-averaging constant false alarm rate (CA-CFAR) algorithm, which is well known in the field of radar detection. We derive exact expressions for the probabilities of detection and false alarm in Rayleigh fading channels. The mean acquisition time of the system under consideration is also derived. The performance of the system is analyzed and compared to that of a hybrid single dwell system.

***Keywords*—**Adaptive threshold, hybrid double-dwell system, CA-CFAR algorithm, DS-CDMA.

I. Introduction

SPREAD spectrum is a means of transmission in which the signal occupies a bandwidth in excess of the minimum necessary bandwidth to send the information. The band spread is accomplished by means of a code which is independent of the data, and a synchronized reception with the code at the receiver is used for dispreading, and subsequently recovers the data. In the last decade a major focus has shifted the applications of spread spectrum systems from military to the commercial arena because of low probability of intercept, multiple user access communications, and the ability to combat jamming and interferences. One basic limitation in DS-CDMA systems is the synchronization time to align the local despreading pseudonoise (PN) code sequence with the incoming spreading PN sequence. The synchronization process generally consists of two steps labeled acquisition (coarse alignment within a fraction of the chip duration) and tracking (fine alignment). Code acquisition is the most challenging task in a spread spectrum receiver. According to the search mode, the code acquisition methods can be classified into three schemes; namely, the serial, hybrid parallel and totally parallel systems. The serial search scheme [1] has the advantage of simple hardware, but the acquisition time is very long for a long PN sequence period. For a long PN sequence period, the totally parallel search [2] has the fastest acquisition time, but the hardware complexity (that is, the number of detectors) increases to the order of the code period. Thus, a trade-off between the acquisition speed and the implementation complexity, a hybrid parallel search scheme [3], [4] has been proposed as an alternative solution.

The correlation between the received and the local codes can be performed sequentially or concurrently [1]. In the first case, an active correlator computes the correlation on a chip-by-chip basis (i.e., serially), while in the second case a passive matched filter code correlates a number of chips in parallel [5]. These approaches can be classified according to the speed required to form the decision variable. In terms of speed, the matched filter scheme has a better performance that the active correlator [5]. The output of the matched filter is then compared to a threshold value. In [6], Linatti presented several methods for threshold settings in code acquisition of DS spread spectrum signals. He gave comparisons using fixed thresholds, thresholds based on constant false alarm rate (CFAR) criteria, and optimal thresholds in the sense they give the minimum acquisition time. It was shown that the best results are obtained using CFAR algorithms [6], [8], since the threshold value is varied adaptively according to various mobile communication environments. The concept of adaptive CFAR detection is well developed in the field of radar [7].

Recently, the double-dwell search method [8], [9], [10] has received much attention because of its simplicity in hardware implementation and its ability to reduce the mean acquisition time, which is a major factor of performance in DS-CDMA systems, and for the low false locks. The second dwell is usually characterized by a longer integration time and is used to verify the correctness of the decision made by the first dwell, thus avoiding occurrences of false alarms. Hence, the synchro cell (H_1 cell) is declared only after the second stage results in synchro cell detection. A failure to detect a synchro cell at the second-dwell, results in advancing the phase of the local code and repeating the double dwell testing.

The system we propose is combining a double dwell hybrid structure using an adaptive CA-CFAR threshold. The proposed system also adopts antenna diversity, since the diversity techniques are effective in combatting the

Manuscript received March 1, 2007.

The authors are with the Electromagnetism and telecommunication laboratory, Constantine, 25000, Algeria (phone: 213.72006978; fax: 213-34475498; e-mail: k_kemih@yahoo.fr).

detrimental effects of fading channels and multiple access interference (MAI) [10], [11], [12]. They also mitigate the signal impairments caused by angular orientation and multipath radio propagation that is to improve the signal to noise ratio (SNR) and maximize the probability of detection. In Section 2, we describe the proposed acquisition system. In Section 3, we derive the expressions of the probabilities of detection, false alarm, and the miss. The mean acquisition time is also determined. Numerical results along with a discussion are presented in Section 4. The conclusions and performance of the proposed system are given in Section 5.

II. System Description

The proposed adaptive double-dwell hybrid PN code acquisition scheme for DS-CDMA with antenna diversity is shown in Fig. 1. The system consists of L antenna elements. The distance between the antenna elements is half the wavelength of the carrier signal. Each antenna element is followed by M correlators in a parallel structure. Each antenna element receives a signal including original data, the PN sequence, as well as noise plus interferences. The outputs are correlated at (LxM) correlators, using locally generated different code phases, and summed to be used as inputs to the adaptive detectors AD1 and AD2. The summed outputs are given by

$$U_m = \sum_{l=1}^{L} X_{lm} \qquad m=1, 2, \ldots, M \tag{1}$$

where M is the number of parallel correlators in each antenna. The first and second adaptive detectors have structures as in Fig.2. For the adaptive operation of the decision processor, the cell-averaging constant false alarm rate (CA-CFAR) algorithm [6] is used from among several CFAR algorithms due to its low hardware complexity. Therefore, the threshold value of the comparator of the j-th branch j=1, 2, …, M is determined based on the sum of all the other branch outputs Z_j, where Z_j is given by

$$Zj = \sum_{m=1, m\neq j}^{M} Um \qquad j=1, 2, \ldots, M \tag{2}$$

and then scaled by T derived from the false alarm rate in accordance with the magnitude of the other branches, using CFAR algorithm [7]. This scaled value Z_jT is compared with the branch input U_j. The threshold can be set adaptively according to the input signals and maintain a constant false alarm rate. If all the inputs of the two adaptive detectors do not exceed each threshold Z_jT, or more inputs exceed the threshold value, the correlators update their code phase by ΔT_c and re-correlate with the received signal. The difference between each detector is its correlation tap size. Generally, the correlation tap size of the first AD is short, whereas that of the second AD2 is long due to considerations of the mean acquisition time and the detection probability, i.e. $N_1 < N_2$ where N_1 and N_2 are the correlation tap sizes of the first and second detectors respectively. By constructing the adaptive detectors in this manner, the acquisition system can reject cells which are not in phase quickly. If the first adaptive detector AD1 indicates that the present cell is the correct cell, then the second adaptive detector AD2 starts working. Also, if the second AD indicates synchronization, then the decision to stop working is taken. In contrast, if one of the detectors fails to indicate that the present cell is correct, the relative time delay of the local PN signal is retarded by ΔT_c, where T_c is the chip time of the PN code and Δ is the code phase updated step. Δ is generally selected to be 0.5 or 1 because synchronization is formed within one chip time interval [13].

Every m-th correlator in the L-th antenna array checks the m-th subregion with the same phase as shown in Fig. 3. Each subregion is obtained by dividing the whole uncertainty region L_c by M. Therefore, it takes L_p iterations to search the whole uncertainty region, where

$$L_p = \frac{\lceil L_c \rceil}{M} \tag{3}$$

Where $[x]$ denotes a minimum integer value greater than or equal to x, and L_c is the length of the PN sequence (code uncertainty region).

III. Analysis of the System

In this paper, frequency-selective Rayleigh fading channel is used, where the fading is sufficiently slow to guarantee that the amplitude of the chips over the correlation interval fades identically [14]. Under the following assumptions [2], we derive formulas of detection probability, false alarm rate and miss detection probability of the proposed system:

- There is only one sample corresponding to the correct phase (one H_1 cell only).
- The outputs of each correlator are independent, because M correlators check different phases.
- If two or more correlators declare synchronization, the system ignores the current phase and checks the next phase.
- The system uses I-Q matched filter correlators.
- The correlation tap sizes $N_i \gg 1$, i =1, 2 are selected such that the correlation of the received sequence and local is about zero when they are not in phase (H_0 cells).
- The uncertainty region is the full code length L_c.
- There is no frequency error.
- The received signal is there given by

$$r(t) = \Re\left\{\sqrt{2P}\alpha(t)c_k(t)h(t - KT_c - \tau)exp\left[j(w_c t + \theta(t)\right]\right\} + n(t) \tag{4}$$

Where,

$\Re$ operation of taking the real part;
P transmit power;
$\alpha(t)$ and $\theta(t)$ gain and phase of the fading channel, respectively;
c_k PN sequence with period L;
$h(t)$ shaping function;
T_c chip duration;
τ code phase to be estimated;

ω_c carrier frequency;
$n(t)$ additive white Gaussian noise with one-sided power spectral density of N_0 watts/HZ.

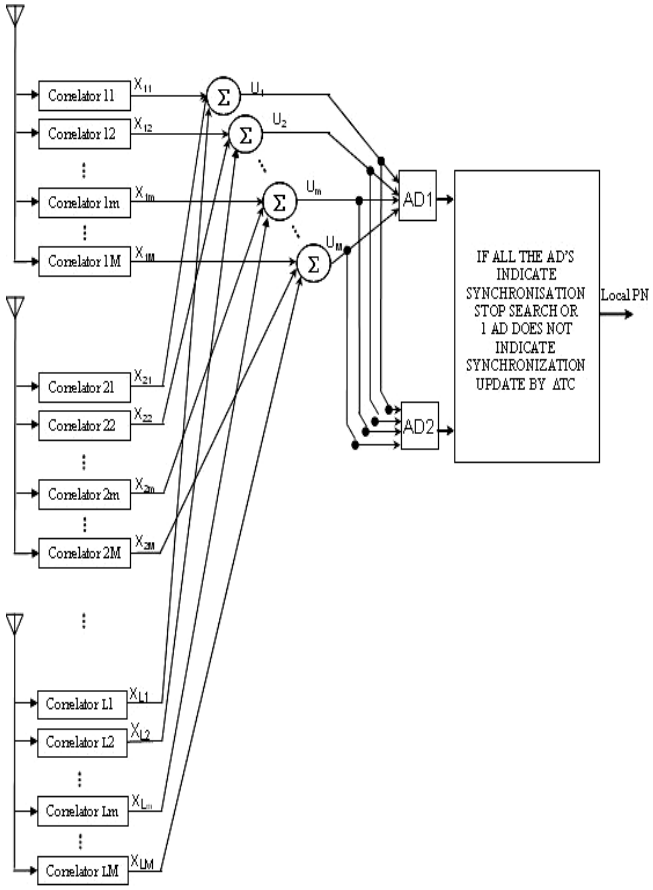

Fig. 1 Block diagram of the proposed system

The code acquisition system based on passive correlators is shown in Fig. 4. The received signal, after I-Q down conversion, chip matching and sampling, is digitally correlated with the local PN code. The structure of the matched filter shown in Fig. 4 is illustrated in Fig. 5.

When a non-coherent reception of Rayleigh faded signal is considered, the probability density function (pdf) of sample H_1, $\mathrm{PR(x/H1)}$ in the correlator output, X_{lm}, of Fig. 5 can be expressed as [2].

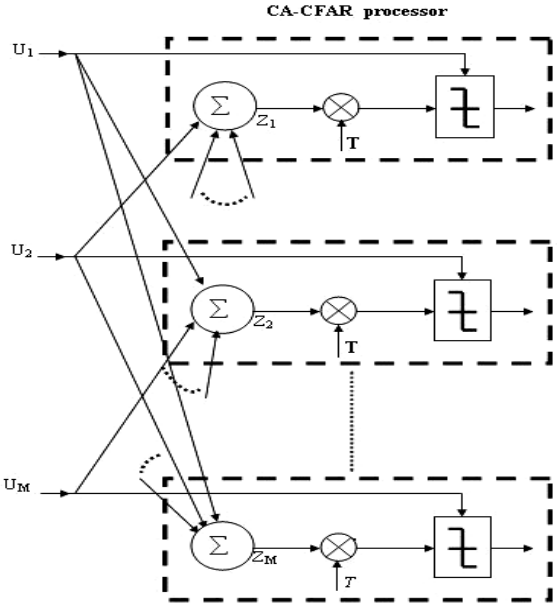

Fig. 2 Adaptive detection block of Fig. 1

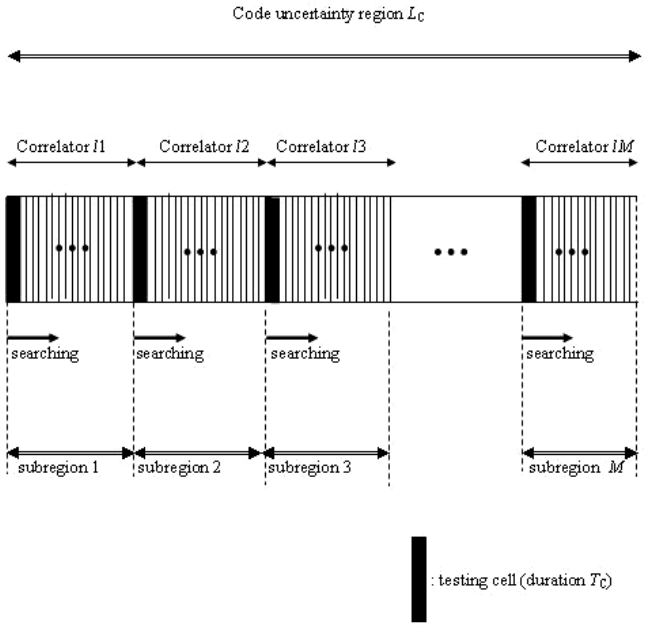

Fig. 3 Searching scheme for the proposed system

$$\mathrm{P}\,R(x/H_1) = \frac{1}{1+\mu} e^{\frac{-x}{1+\mu}} = G(1,1+\mu) \tag{5}$$

and the pdf of sample H_0 is

$$\mathrm{P}R(x/H_0) = e^{-x} = G(1,1) \tag{6}$$

where, μ denotes the average SNR and $G(.)$ is the Gamma distribution. Therefore, the pdfs of U_m, m =1, 2, …, M, in Fig. 1 are

$$\mathrm{P}R(u/H_1)=\frac{1}{\Gamma(L)(1+\mu)^L}u^{L-1}e^{\frac{-u}{1+\mu}} \quad (7)$$

and

$$\mathrm{P}R(u/H_0)=\frac{1}{\Gamma(L)}u^{L-1}e^{-u} \quad (8)$$

where Γ(.) means the Gamma function. To determine the threshold value of the m-th CA-CFAR processor, the system sums all the branch outputs except for the tested branch. In the CA-CFAR algorithm, all the signals except for the test signal are assumed ton be noise [6], the pdf of the values U_j, $j \neq m$, j =1, 2, …, M, is the same as $\mathrm{P}_U(u/H_0)$. The pdf $\mathrm{P}_U(u/H_0)$ can be also expressed as $G(L,1)$. The pdf of Z_m, $\mathrm{P}_Z(z)$, is

$$\mathrm{P}_Z(Z)=\frac{1}{\Gamma(L(M-1))}Z^{L(M-1)-1}e^{-x} \quad (9)$$

where, Z_m is the m-th branch sum of the outputs of the other (M-1) branches.

With the CA-CFAR algorithm, the detection probability of the i-th, i=1, 2, AD, P_{Di} is

$$\mathrm{P}_{Di}=\int_0^\infty P_Z(z)\int_{T_i x}^\infty P_U(u/H_1)dudz\times\left[\int_0^\infty P_Z(z)\int_0^{T_i z}P_U(u/H_0)dudz\right]^{M-1}$$
$$=A_i(1+\mu)\left[1-A_i(1)\right]^{M-1} \quad (10)$$

where,

$$A_i(\alpha)=\frac{1}{\Gamma(L(M-1))}\times\sum_{k=0}^{L-1}\frac{1}{k!}\left(\frac{Ti}{\alpha}\right)^k\frac{(L(M-1)-1+k)!}{\left(\frac{Ti}{\alpha}\right)^{L(M-1)+k}} \quad (11)$$

The false alarm rate, P_{FA}, of the proposed system can be divided into two cases; P_{FA/H_1} and P_{FA/H_0}. P_{FA/H_1} is the case that one of (M-1) H_0 cells exceeds the threshold value when there is exists one H_1 cell whose value is less than the threshold. P_{FA/H_0} is the case that one of M H_0 exceeds the threshold value. Hence,

$$P_{FA_1/H_1}=\int_0^\infty P_Z(Z)\int_{T_iZ}^\infty P_U(u/H_0)dudZ\times\left[\int_0^\infty P_Z(z)\int_0^{T_iZ}P_U(u/H_1)dudz\times\int_0^\infty P_Z(Z)\int_0^{T_iZ}P_U(u/H_0)dudz\right]^{M-2}$$
$$=A_i(1)\left[1-A_i(1+\mu)\right]\left[1-A_i(1)\right]^{M-2} \quad (12)$$

$$P_{FA_i/H_0}=\int_0^\infty P_Z(Z)\int_{T_iZ}^\infty P_U(u/H_0)dudZ\times\left[\int_0^\infty P_Z(Z)\int_0^{T_iZ}P_U(u/H_0)dudZ\right]^{M-1}$$
$$=A_i(1)\left[1-A_i(1)\right]^{M-1} \quad (13)$$

Since the correlator outputs of the first and second ADs are independent, the detection probability of the system is the product of each AD's detection probability. Hence, the probability of actually detecting the correct cell is

$$P_{D_i}=P_{D_1}\cdot P_{D_2} \quad (14)$$

The false alarm of the system when (M-1) H_0 cells exceed the threshold is

$$P_{FA/H_1}=P_{FA_1/H_1}\cdot P_{FA_2/H_1} \quad (15)$$

When M H_0 cells exceed the threshold, the false alarm is

$$P_{FA/H_0}=P_{FA_1/H_0}\cdot P_{FA_2/H_0} \quad (16)$$

We notice that P_{FA/H_0} appears (L_p -1), while P_{FA/H_1} occurs once in the L_p iterations, since there exists one H_1 cell in the uncertainty region. As a result, P_{FA} is rarely affected by P_{FA/H_1}, despite the fact that it depends on the SNR. Therefore, the false alarm of the proposed system is

$$P_{FA}=\frac{1}{L_p}P_{FA/H_1}+\frac{L_p-1}{L_p}P_{FA/H_0} \quad (17)$$

The acquisition process can be represented by a signal flow graph [1]. The flow diagram of the proposed double-dwell hybrid system is shown in Fig. 6. Let assign more general gains $H(z)$ to the different branches of the model in Fig. 6 as follows : $H_D(z)$ is the gain of branch leading from node H_1 (L_p–th) to the node ACQ ; $H_M(z)$ is the gain of the branch connecting H_1 with node 1, while $H_I(z)$ is the gain of the branch connecting any other two successive nodes (i,i+1) ; i= 1, 2, …, L_p -1. Furthermore, the process can move between any successive nodes(i,i+1) with $i \neq L_p$ either without false alarm (FA) associated with $H_{NFA}(z)$ or by first reaching the false alarm state (branch gain $H_{FA}(z)$), then pass from FA to node i+1. $H_{NFA}(z)$ models all paths between successive H_0 states which do not lead to the false tracking-loop ; the latter path is modeled by $H_{FA}(z)$. Similarly, both $H_D(z)$ and $H_M(z)$ include all paths leading to successful acquisition or miss, respectively. From the state diagram illustrated in Fig. 6, we can see that the miss probability P_M is related to both P_D and P_{FA/H_1}. Accordingly, P_M is given by

$$P_M=1-P_D-P_{FA/H_1} \quad (18)$$

The mean acquisition time of the proposed system can be obtained from the state diagram [14]

$$E[T_{acq}]=\left.\frac{dH(z)}{dz}\right|_{z=1} \quad (19)$$

Where, $H(z)$ is the generating function of the state diagram .

In deriving the mean acquisition time, we take in account the following assumptions:

1- The probability of starting at each node is equal, with a uniform distribution of the incoming PN.

2- A start at the correct phase node, 'state1', is excluded.

The gains of different branches are as follows.

$$H_D(z)=P_{D_1}\cdot P_{D_2}z^{(N_1+N_2)T_c} \quad (20)$$

$$H_{FA_1}(z) = P_{FA_1/H_1} \cdot P_{FA_2/H_1} z^{(N_1+N_2)T_c} \quad (21)$$

$$H_{FA_0}(z) = P_{FA_1/H_0} \cdot P_{FA_2/H_0} z^{(N_1+N_2)T_c} \quad (22)$$

$$H_M(z) = P_{M_1} z^{N_1T_c} + P_{D_1}(1-P_{D_2}) z^{(N_1+N_2)T_c} + P_{FA_1/H_1}(1-P_{FA_2/H_1}) z^{(N_1+N_2)T_c} \quad (23)$$

$$H_R(z) = z^{K(N_1+N_2)T_c} \quad (24)$$

$$H_{NFA}(z) = \left[(1-P_{FA_1/H_0}) + P_{FA_1/H_0}(1-P_{FA_2/H_0}) z^{N_2T_c}\right] z^{N_1T_c} \quad (25)$$

$$H_T(z) = H_{NFA}(z) + H_{FA_0}(z).H_R(z) \quad (26)$$

The gain of the state diagram is given by

$$H(z) = H_D(z)\left[1 - \left\{H_M(z) + H_{FA_1}(z).H_R(z)\right\} H_T(z)^{Lp-1}\right]^{-1} \times \sum_{i=1}^{Lp} \frac{1}{L_p} \left\{H_T(z)\right\}^{L_p-i} \quad (27)$$

From the branch gains in (20)-(26), the transfer function (27) and the equation (19), the mean acquisition time can be induced as [13]

$$E[T_{acq}] = \frac{(N_1+N_2)T_c}{P_{D_1} \cdot P_{D_2}} \begin{bmatrix} K\, P_{FA_1/H_1} P_{FA_2/H_1} + P_{FA_1/H_1}(L_p-1) \\ (1+K\, P_{FA_1/H_0})(\frac{3}{2} - P_{D_1} P_{D_2}) \end{bmatrix} + \frac{N_1T_c}{P_{D_1} \cdot P_{D_2}} \left[1 + (L_p-1)(1-P_{FA_1/H_0})(\frac{3}{2} - P_{D_1} P_{D_2})\right] + \frac{N_2T_c}{P_{D_1} \cdot P_{D_2}} \left[P_{D_1} + P_{FA_1/H_1}\right] \quad (28)$$

IV. Numerical Result

To study the performance of the system suggested, we determine its probability of detection, as well as the mean acquisition time according to several parameters in a frequency-selective Rayleigh channel. The results obtained are compared to a single-dwell hybrid adaptive system.

For the analysis, the false alarm was set to 10^{-6} and the length of the PN code, L_c, was set to 2560. The chip time, T_c, and the penalty time constant, K, were set at 3.84 Mbps and 10000, respectively. The probability of detection of the system according to the number of used antennas is shown in Fig. 7 when the number of correlators is fixed at 30, and the durations of the correlations of both dwells are 128, and 256 respectively. This probability increases with the number of antennas. In Fig. 8, we have fixed the number of antennas at 3, and the durations of correlations to 128, and 256.We note that the probability of detection increases with the number of correlators. The probability of detection also increases with the durations of the correlations, as shown in Fig. 9, where the number of antennas was fixed at 3, and the number of correlators at 30.

To show the improvement made by the system suggested, we have carried out a comparative study with a single-dwell hybrid adaptive system, based on the criterion of the mean acquisition time, and the probability of detection. This comparison is illustrated by Fig. 10, where we have calculated the probability of detection of the two systems when the number of antennas is 3, the number of the correlators is 30, the duration of correlation of the first system is fixed at 128, and the durations of correlation of both dwells of the system suggested are 128, and 256 respectively. The result obtained shows that the probability of detection of the system suggested is better than that of the system with simple dwell under the conditions where the SNR is weak.

The mean acquisition time of the system is presented in Fig. 11 according to the durations of correlation, where the number of antennas was fixed at 3 and the number of correlators was 20. It is noticed that with two antennas, the mean acquisition time is lower than that of the system using only one antenna, when the SNR is lower than -10dB, which confirms that when the SNR is better, the mean acquisition time is independent of the number of antennas. We can also note that the mean acquisition time is inversely proportional to the durations of correlation of both dwells.

A comparison of the mean acquisition time between the system suggested, and the system with simple dwell is given by Fig. 13, according to the durations of correlation. We considered three antennas; each one was followed by 30 correlators. According to Fig. 11, the mean acquisition time of the system with simple dwell is higher than that of the system suggested for all the values of the SNR. We can also notice that the performance of the system with simple dwell improves when the SNR exceeds -5 dB.

V. Conclusion

In this paper, we analyzed the performance of an hybrid double-dwell system with antenna diversity by adopting the CA-CFAR algorithm to the acquisition process in DS-CDMA communication systems, then we compared its performance to a single-dwell hybrid system by deriving formulas of the probabilities of detection, false alarm, and the miss detection, then, the mean acquisition time of the proposed system in frequency-selective Rayleigh fading channels. The detection probability of the proposed system increased with the increasing of the number of antennas, the correlation tap sizes of the two dwells, and the branch size of the correlator. The proposed system presents more performance than a single-dwell system, especially for environment with low SNR, where its probability of detection was higher while maintaining a constant false alarm rate, since double-dwell systems guarantee low false locks. The proposed system is able to produce robust performance in the mean acquisition time regardless of the surroundings.

REFERENCES

[1] Polydoros and C. L. Weber, "A unified approach to serial search spread-spectrum code acquisition-Part I : General theory," *IEEE Transaction Communication*, vol.COM-32, no.5, May 1984.

[2] E. A. Sourour, S. C. Gupta, "Direct-sequence spread-spectrum parallel acquisition in a fading mobile channel, "*IEEE Transaction communication*, vol.COM-38, no. 7, July 1990.

[3] C. Baum and V. Veeravalli, "Hybrid acquisition schemes for direct sequence CDMA systems," *IEEE, International Conference on Communications*, 1994, vol. 3, pp. 1433-1437.

[4] W. Zhuang, "Noncoherent hybrid parallel PN code acquisition for CDMA mobile communications," *IEEE Transaction on Vehicular Technology*, vol. 45, no. 4, p. 643-656, 1996.

[5] Polydoros, and C. L. Weber," A unified approach to serial search spread spectrum code acquisition-Part II: A matched filter receiver," IEEE Transaction Communication, vol. 32, no. 5, pp. 550-560, May 1994.

[6] J. Linatti, "On the threshold setting principles in code acquisition of DS-SS signals," *IEEE Journal on Selected Areas in Communications*, vol.18, no.1, p. 62-72, January 2000.

[7] H. Oh, D. Han, and C. Kim, "An environmental robust PN code acquisition architecture in DS-CDMA systems," *CIC 2000*, vol, , Seoul, Korea, Nov 2000, pp. 201-205.

[8] H. Kim, I. Song, Y. Lee, S. Kim, and Y. Kim, "Double-dwell serial-search PN code acquisition using a non parametric detection in DS/CDMA systems," MILCOM 1999-*IEEE Military Communications Conference*, no.1, October 1999, pp.571-574.

[9] D.M. Dicarlo, and C.L. Weber, "Multiple dwell serial acquisition of direct sequence signals acquisition," *IEEE Transaction Communication*, vol. 31, no. 5, p. 650-659, 1983.

[10] R. Rick and L. Milstein, "Parallel acquisition of spread-spectrum signals with antenna diversity," *IEEE Transaction Communication*, vol. COM-45, no. 8, p. 903-905, 1997.

[11] Y. Tokgoz, B. D. Rao, M. Wengler, and B. Judson, "Performance analysis of optimum combining in antenna array systems with multiple interferers in flat Rayleigh fading," *IEEE Transaction communication*, vol. 52, no. 7, pp. 1047-1050, July 2004.

[12] H. Sock, C. Hyun, and D. Seog, "Adaptive hybrid PN code acquisition with antenna diversity in DS-CDMA systems," *IEEE Transaction Communication*, vol. E85-B. no. 4, p. 716-721, April 2002.

[13] Viterbi, CDMA principles of spread spectrum communication, Addison-Wesley, Massachusetts, 1995.

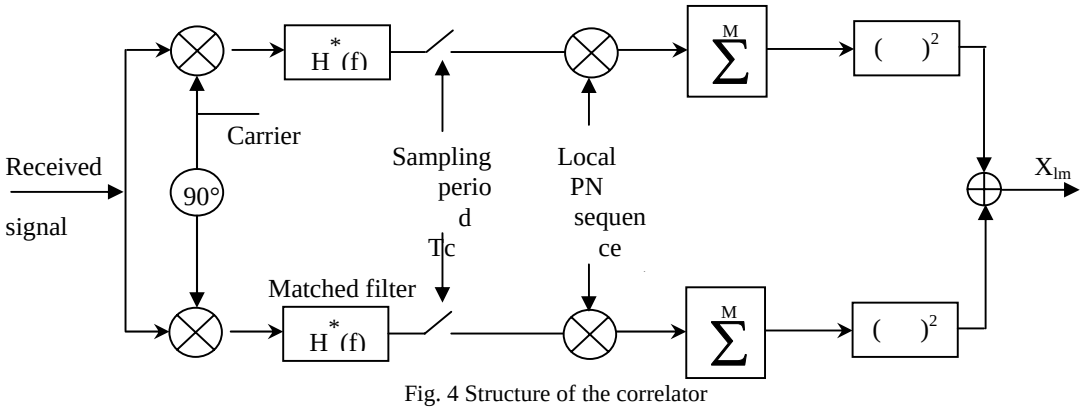

Fig. 4 Structure of the correlator

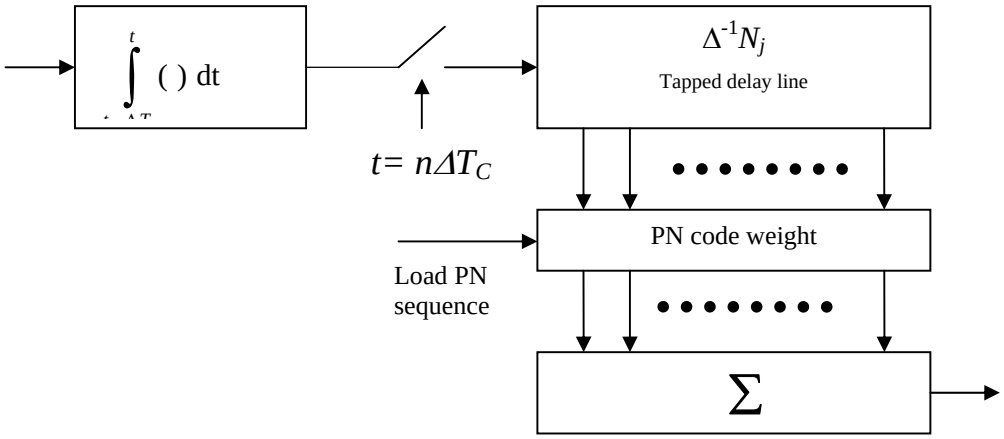

Fig. 5 Matched filter correlator of Fig. 4

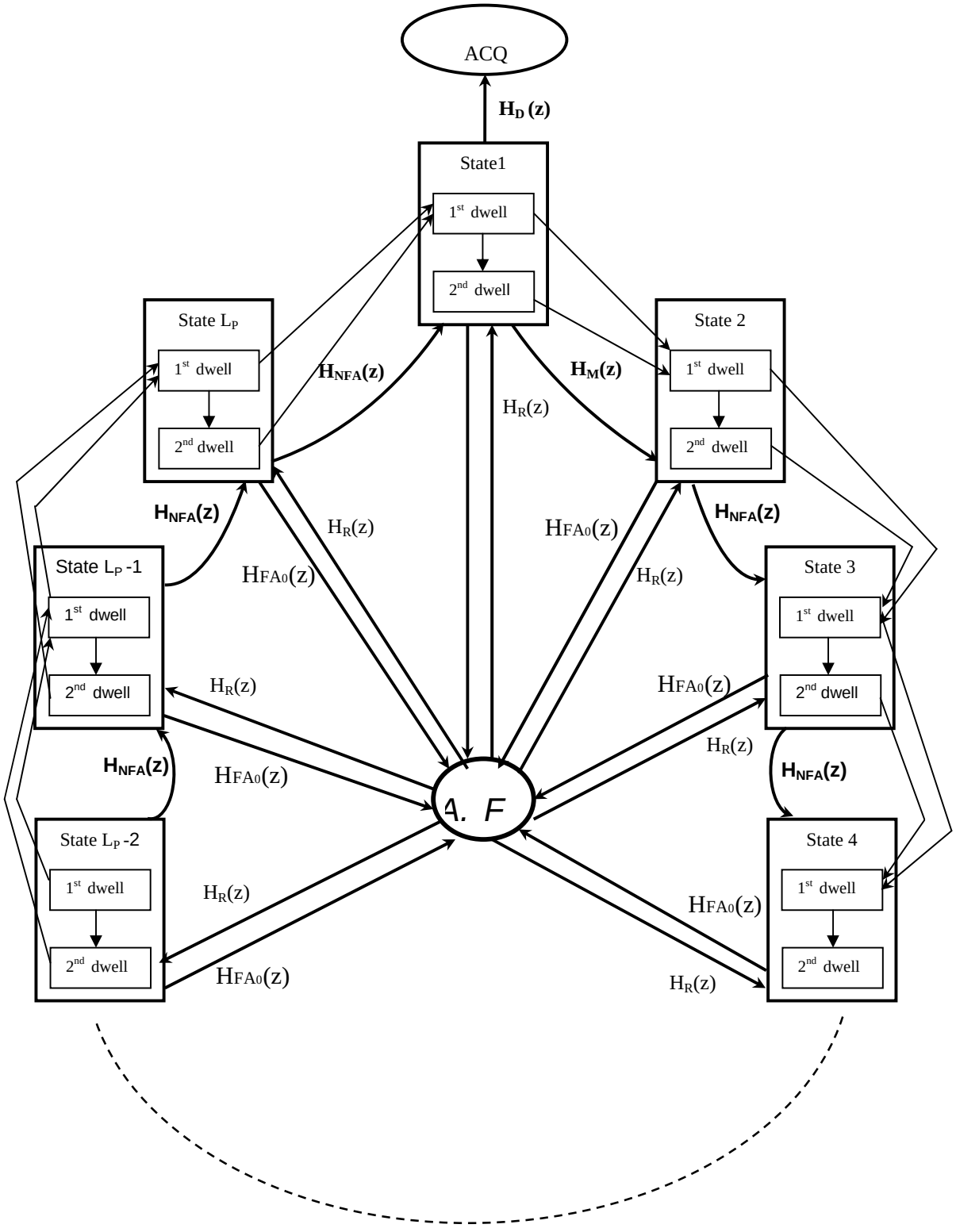

Fig. 6 Flow diagram of the proposed system

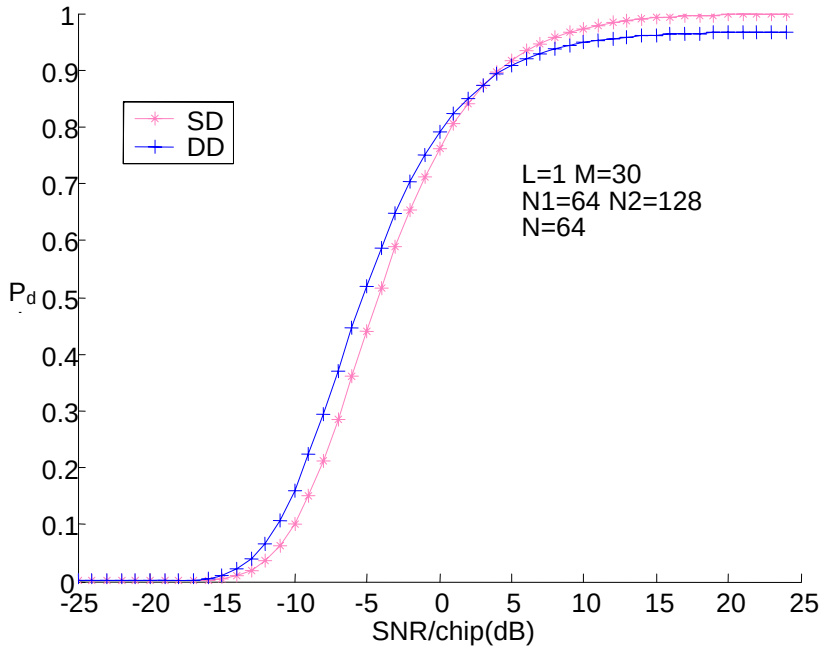

Fig. 7 The probability of detection according to the SNR/Chip, when M=30, N_1=128 et N_2=256

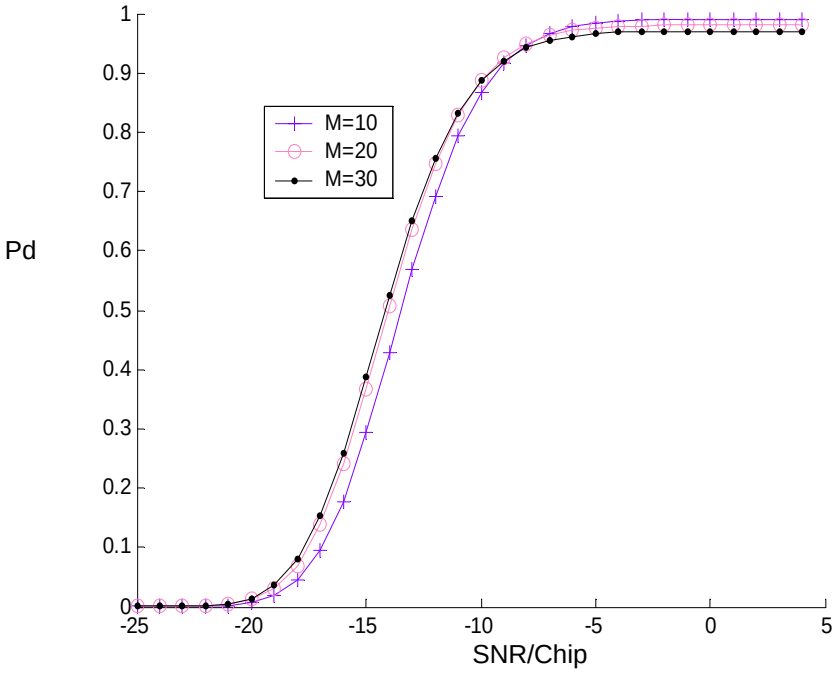

Fig. 8 The probability of detection according to the SNR/Chip, when L=3, N_1=128 and N_2=256

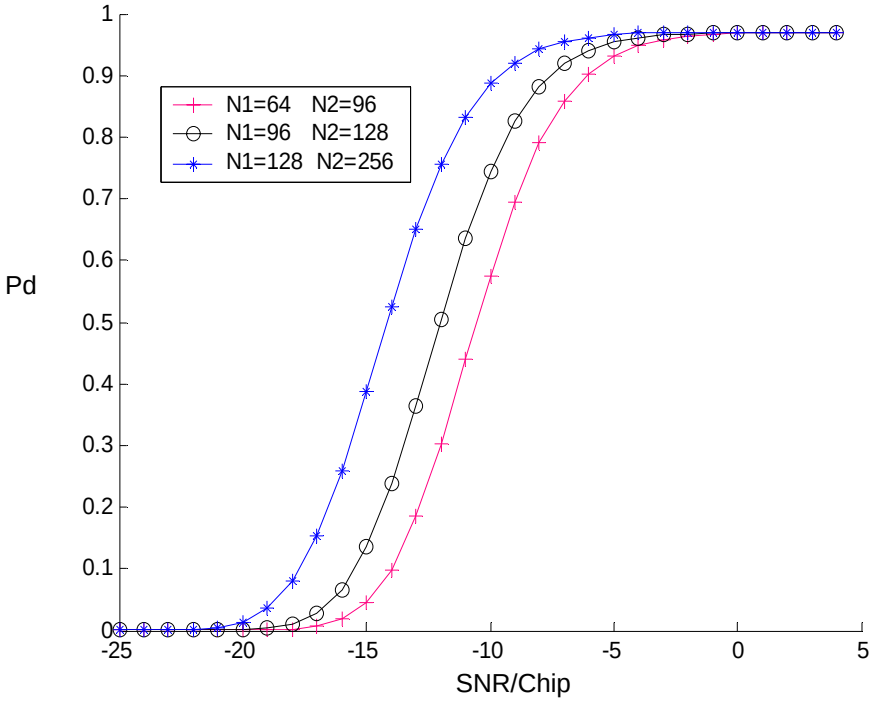

Fig. 9 The probability of detection according to the SNR/Chip, when L=3 and M=30

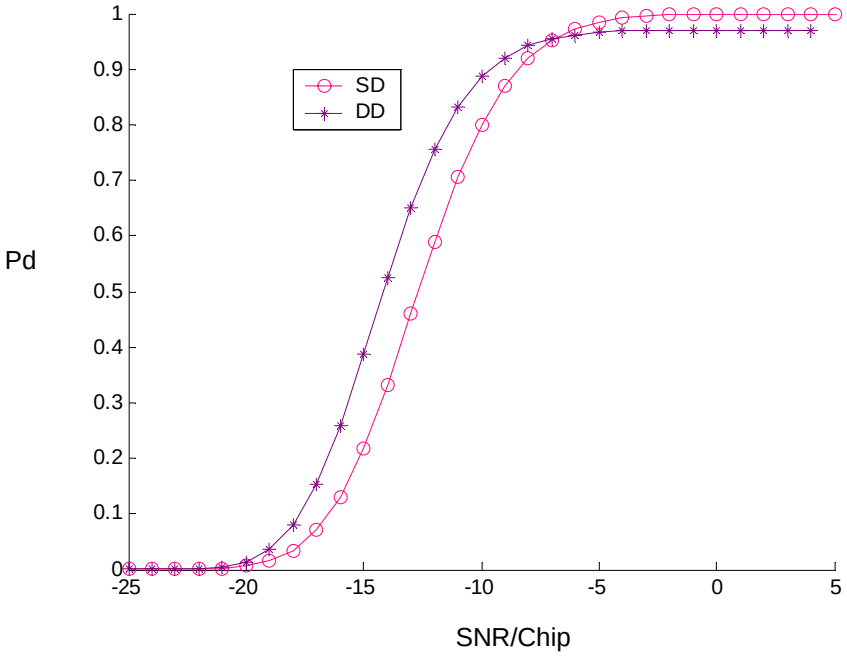

Fig. 10 Comparison of the probabilities of detection of the two systems according to the SNR/Chip, when L=3, M=30, N=128, N_1=128 and N_2=256

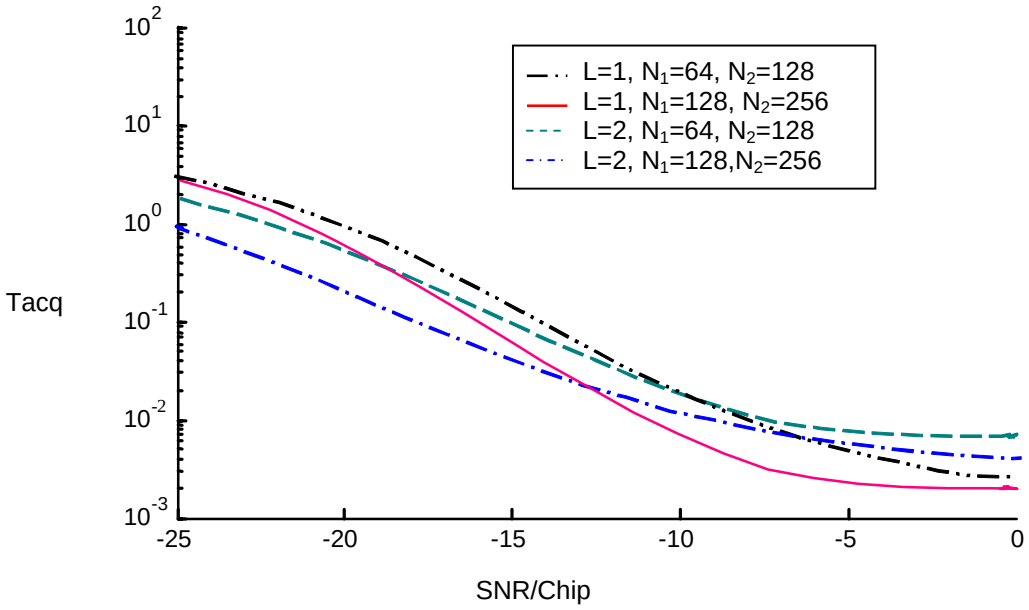

Fig. 11 The mean acquisition time of the system according to the SNR/Chip, when M=20

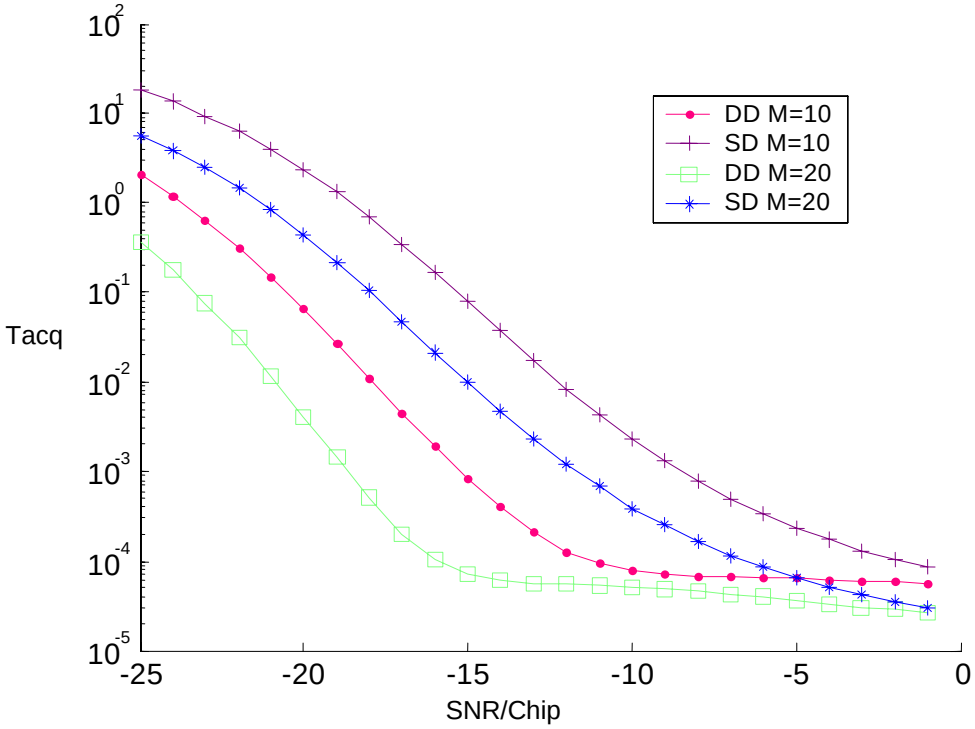

Fig. 12 Comparison of the mean acquisition times of the two systems according to the SNR/Chip, when L=3, N=128, N_1=128 et N_2=256